ASTRONOMY & ASTROPHYSICS
SUPPLEMENT SERIES

JANUARY **1995**, PAGE 193

Astron. Astrophys. Suppl. Ser. **109**, 193-197 (1995)

Atomic data from the IRON Project. VIII. Electron excitation of the $3d^4\ ^5D_J$ ground state fine-structure transitions in Ti-like ions V II, Cr III, Mn IV, Fe V, Co VI and Ni VII*

K.A. Berrington

Department of Applied Mathematics & Theoretical Physics, The Queen's University, Belfast, BT7 1NN, UK

Received July 11; accepted September 6, 1994

Abstract. — Electron excitation collision strengths for the $3d^4\ ^5D_{J-J'}$ ground term fine-structure transitions in titanium-like ions V II, Cr III, Mn IV, Fe V, Co VI and Ni VII are calculated using R-matrix techniques. The model target ion includes all $3d^4$ terms, and the low-energy collision strengths are dominated by autoionizing resonances. The collision strength is averaged over a Maxwellian velocity distribution to obtain effective collision strengths as a function of electron temperature. To our knowledge, these are the first published data for these processes.

Key words: atomic data

1. Introduction

New astronomical observations are revealing the presence of trace metals in many types of astronomical objects. For example, high-dispersion IUE observations of the brightest of the hot stars showed absorption features from photospheric Fe, Ni and possibly Cr (Holberg et al. 1993); identifications included Ti-like Fe V, and Ni became the second iron group element to be positively identified in the photospheres of the hot DA white dwarfs (Holberg et al. 1994). Adelman et al. (1993) have analysed the abundances of elements such as Cr, Mn, Fe, Co and Ni in early type stars from IUE high-dispersion spectrograms. Lindley (1991) reported Hubble Space Telescope detections of lines due to metal ions in the spectra of χ Lupi; identifications include Ti-like V II. Also from HST observations, Federman et al. (1993) have observed weak interstellar lines, including Ni and the first interstellar detection of Co. In the infrared, Li et al. 1993 have analysed emission lines of Fe, Co and Ni ions in SN 1987A.

Metal ions in the titanium isoelectronic sequence are possible emitters of infrared lines since their ground configuration $3D^4\ ^5D_J$ gives rise to five fine-structure levels (J=0, 1, 2, 3 and 4). However, to our knowledge, there are no available data for the electron excitation of these levels: the bibliographic surveys by Pradhan & Gallagher (1992), and by Itikawa (1990, 1992) do not contain any references for these ions. The present calculation is to rectify this situation, and is part of an international collaboration known as the IRON Project (Hummer et al. 1993, refered to as Paper I) to obtain accurate collision rates for fine-structure transitions.

Other papers in the IRON project series include: the calculation of effective collision strengths for infrared transitions in C-like ions (Lennon & Burke 1994, Paper II), B-like ions (Zhang et al. 1994, Paper III), F-like ions (Saraph & Tully 1994, Paper IV), O-like ions (Butler & Zeippen 1994, Paper V), Fe II (Zhang & Pradhan 1994, Paper VI); radiative transition probabilities for Fe II (Nahar 1994, Paper VII).

2. The calculation

The basic atomic theory, the approximations and the computer codes employed in the IRON Project are described in Paper I. Two calculations were performed for each ion.

The first calculation was carried out in LS coupling; collision strengths for fine-structure transitions obtained using an algebraic transformation to intermediate coupling, as described in Sect. 2.6 of Paper I; the so-called JAJOM approach (Saraph 1978). This procedure makes no allowance for the fine-structure splitting of the terms, and will therefore be accurate only at scattering energies

*Table 2 is available electronically via anonymous ftp 130.79.128.5 et the CDS

above the fine-structure thresholds; the JAJOM approach was therefore used at the higher energies.

In this calculation, all 16 LS terms associated with the $3d^4$ configuration were included in the target expansion, as in the corresponding Opacity Project calculation (Sawey & Berrington 1992). The target wavefunctions were constructed from 1s, 2s, 2p, 3s, 3p and 3d orbitals as given by Clementi & Roetti (1974).

The second calculation included the same 16 LS terms, but used the Breit-Pauli formulation of the R-matrix method, again described in Paper I. Fine-structure splitting was therefore included ab initio, and the scattering results should be highly accurate. However the procedure is computationally much more demanding than the JAJOM approach, so it was used only at the lowest scattering energies, below the first excited term threshold, where the effects of fine-structure splitting are likely to be significant.

In this latter calculation, all 34 fine-structure levels associated with the $3d^4$ configuration were explicitly included in the total wavefunction. The threshold energies for the five levels associated with the ^5D ground state term are displayed in Table 1. It should be noted that the Breit-Pauli approach used in the present R-matrix calculations only includes the one-body spin-orbit, mass-correction and Darwin terms in the Hamiltonian; two-body terms for example are omitted. This limitation would affect the accuracy of the calculated level energies. Shown for comparison in Table 1 are values from other published sources; however, no adjustment was made in the present calculations to account for the differences.

Table 1. Fine-structure energy levels of the $3d^4\ ^5D_J$ ground state in Ti-like ions, in Rydberg units. The first row for each ion contains the theoretical energies from the current Breit-Pauli calculation; the second row is from the following tabulations: (1) Moore (1971), (2) Sugar & Corliss (1977), (3) Corliss & Sugar (1977), (4) Reader & Sugar (1975), (5) Corliss & Sugar (1981)

	J=0	J=1	J=2	J=3	J=4
V II	.0	.00041	.00123	.00242	.00397
(1)	.0	.00033	.00097	.00190	.00309
Cr III	.0	.00068	.00201	.00396	.00647
(2)	.0	.00057	.00167	.00325	.00525
Mn IV	.0	.00103	.00303	.00595	.00967
(3)	.0	.00090	.00261	.00503	.00807
Fe V	.0	.0015	.0044	.0085	.0137
(4)	.0	.0013	.0038	.0073	.0117
Co VI	.0	.0021	.0060	.0117	.0187
(1)	.0	.0019	.0053	.0103	.0163
Ni VII	.0	.0028	.0081	.0156	.0249
(5)	.0	.0025	.0073	.0139	.0218

3. Results

Collision strengths were computed for each ion for the required fine-structure transitions over a sufficiently wide and fine energy mesh, in order to be able to integrate over a Maxwellian distribution to obtain the *effective collision strength*, from which the excitation and de-excitation rate coefficients can easily be obtained (Paper I).

As already stated, two methods were used for each ion: the Breit-Pauli procedure, and the 'JAJOM' procedure. Shown in Fig. 1 is a comparison of the collision strength for $^5D_{0-1}$ in Fe V obtained from the two methods, at energies below the first excited term threshold. The collision strength is clearly dominated by resonances; the position and width of these resonances, particularly close to threshold, can have a marked effect on the thermal average at low temperatures. It can be seen from the figure that resonances are both shifted and split in the Breit-Pauli procedure. Further, the threshold is not at zero energy in the Breit-Pauli calculation, because of fine-structure splitting; but in the 'JAJOM' approach the fine-structure thresholds are assumed to be degenerate, and this clearly affects the near-threshold resonances. For this particular transition, the effective collision strength obtained from using 'JAJOM' is 1.164 at 10 000 K, compared with 0.861 in the Breit-Pauli approach. The difference reduces to zero at the highest temperature considered for this ion, 1 000 000 K, indicating the two methods agree at high energies, as expected. Thus, for each ion, the Breit-Pauli approach is used to delineate near-threshold energies, with the computationally less demanding 'JAJOM' being used at higher energies.

Table 2[1] is a tabulation of the effective collision strength for each fine-structure transition in the $3d^4\ ^5D$ ground term for each ion considered. The range of temperatures chosen for each ion was ± 1.0 dex of the temperature of maximum ionic abundance given by Shull & Van Steenberg (1982).

4. Discussion

Collision strengths have been calculated using R-matrix techniques for the $3d^4\ ^5D_{J-J'}$ ground state fine-structure transitions in six Ti-like ions. These appear to be the first such data in the literature, so it is not possible to compare against other workers. However, it is known from other R-matrix calculations on other ions that the method should be reliable, particularly at low energies and temperatures. The most serious limitation of the present work is the omission of any effects due to target states above the $3d^4$ manifold. States such as $3d^3\ 4s$ and $3d^3\ 4p$ will give resonance structures below their thresholds, and at higher energies channel coupling effects, particularly with the odd-parity 4p states, would be important. Of the ions

[1]Table 2 is available in electronic form via an anonymous ftp copy at the CDS.

considered here, V II is likely to be the most seriously affected, as the 4s and 4p states lie so close to the 3d states for that ion. However, these effects should diminish as we ascend the isoelectronic sequence.

From other work by the IRON Project, the accuracy of the effective collision strengths given in Table 2 is estimated to be better than 10% at the lower temperatures, with a greater uncertainty at higher temperatures and for V II.

Acknowledgements. This work was done with the support of an SERC grant GR/H93576, and an EC network contract ERB CHRX CT920013.

References

Adelman S.J., Cowley C.R., Leckrone D.S., Roby S.W., Wahlgren G.M. 1993, ApJ 419, 276
Butler K., Zeippen C.J. 1994, A&AS, in press
Clementi E., Roetti C. 1974, Atom. Data Nucl. Data Tables 14, 177
Corliss C., Sugar J. 1977, J. Phys. Chem. Ref. Data 4, 1293
Corliss C., Sugar J. 1981, J. Phys. Chem. Ref. Data 10, 258
Federman S.R., Sheffer Y., Lambert D.L., Gilliland R.L. 1993, ApJ 413, L51
Holberg J.B., Barstow M.A., Buckley D.A.H. et al. 1993, ApJ 416, 806
Holberg J.B., Hubeny I., Barstow M.A. et al. 1994, ApJ 425, L105
Hummer D.G., Berrington K.A., Eissner W. et al., A&A 279, 298 (Paper I)
Itikawa Y. 1990, ISAS RN 459 (The Institute of Space and Astronautical Science, Yoshinodai, Kanagawa 229, Japan)
Itikawa Y. 1992, ISAS RN 512 (The Institute of Space and Astronautical Science, Yoshinodai, Kanagawa 229, Japan)
Lennon D.J., Burke V.M. 1994, A&AS 103, 273
Li H., McCray R., Sunyaev R.A. 1993, ApJ 419, 824
Lindley 1991, Nature 351, 441
Moore C.E. 1971, NSRDS-NBS 35 Vols. I & II
Nahar S.N. 1994, A&A, submitted
Pradhan A.K., Gallagher J.W. 1992, Atom. Data Nucl. Data Tables 52, 227
Reader J., Sugar J. 1975, J. Phys. Chem. Ref. Data 4, 400
Saraph H.E. 1978, Comp. Phys. Commun. 15, 247
Saraph H.E., Tully J.A. 1994, A&AS, in press
Sawey P.M.J., Berrington K.A. 1992, J. Phys. B 25, 1451
Shull J.M., Van Steenberg M. 1982, ApJS 48, 95
Sugar J., Corliss C. 1977, J. Phys. Chem. Ref. Data 6, 343
Zhang H.L., Graziani M., Pradhan A.K. 1994, A&A 283, 319
Zhang H.L., Pradhan A.K. 1994, A&A, submitted

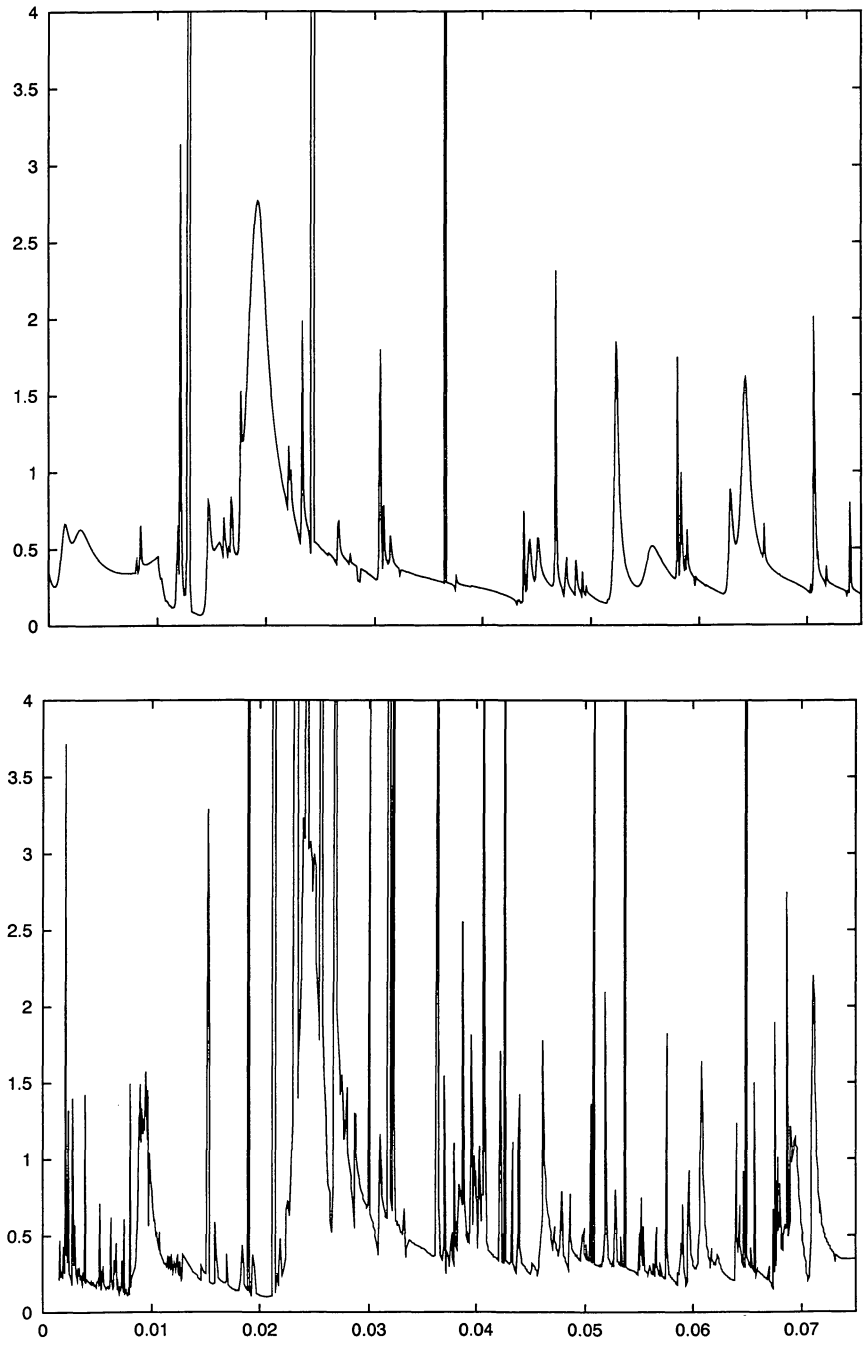

Fig. 1. Collision strength for the $3d^4\ ^5D_{0-1}$ fine-structure transition in Fe v, as a function of electron energy in Rydberg units. The upper plot is the 'JAJOM' method; the lower plot the Breit-Pauli method. The plots show the energy range near the ground state fine-structure thresholds; for reference, the first excited term threshold is at 0.251 Ryd. Note that the thermally averaged effective collision strength in the JAJOM approach is 35% higher than the Breit-Pauli value at 10 000 K

Table 2. Effective collision strengths for $3d^4\ ^5D_{J-J'}$ fine-structure transitions in Ti-like ions. The row containing the ion symbol indicates the values of log T(Kelvin) for that ion. The left-hand column indicates the initial and final J and J' levels

V II	3.0	3.2	3.4	3.6	3.8	4.0	4.2	4.4	4.6	4.8	5.0
0-1	2.031	1.929	1.810	1.723	1.668	1.599	1.486	1.331	1.158	0.996	0.864
0-2	0.545	0.505	0.486	0.507	0.550	0.578	0.570	0.525	0.456	0.385	0.323
0-3	0.488	0.461	0.461	0.501	0.550	0.571	0.549	0.491	0.416	0.340	0.274
0-4	0.183	0.182	0.190	0.210	0.234	0.249	0.250	0.240	0.226	0.211	0.196
1-2	4.352	4.108	3.881	3.773	3.718	3.576	3.295	2.916	2.514	2.151	1.861
1-3	1.477	1.386	1.392	1.548	1.737	1.805	1.712	1.510	1.271	1.050	0.871
1-4	0.779	0.752	0.750	0.793	0.858	0.903	0.902	0.859	0.792	0.719	0.648
2-3	6.023	6.951	8.886	10.64	11.17	10.40	8.895	7.221	5.715	4.517	3.634
2-4	2.147	2.515	3.225	3.817	3.980	3.747	3.292	2.770	2.279	1.867	1.545
3-4	7.366	9.300	12.60	15.01	15.20	13.61	11.26	8.914	6.935	5.420	4.329
Cr III	3.4	3.6	3.8	4.0	4.2	4.4	4.6	4.8	5.0	5.2	5.4
0-1	1.020	1.007	0.993	0.965	0.905	0.815	0.716	0.628	0.562	0.517	0.483
0-2	0.398	0.431	0.470	0.485	0.459	0.402	0.334	0.272	0.225	0.193	0.173
0-3	0.345	0.346	0.369	0.385	0.370	0.327	0.271	0.218	0.174	0.141	0.115
0-4	0.300	0.333	0.383	0.405	0.385	0.338	0.282	0.232	0.191	0.160	0.134
1-2	2.555	2.546	2.571	2.537	2.372	2.101	1.800	1.533	1.330	1.188	1.085
1-3	1.335	1.342	1.392	1.389	1.286	1.108	0.911	0.738	0.603	0.506	0.436
1-4	0.991	1.113	1.284	1.359	1.290	1.124	0.930	0.750	0.613	0.505	0.418
2-3	4.410	4.190	4.059	3.850	3.485	3.022	2.565	2.185	1.905	1.714	1.574
2-4	1.843	2.019	2.289	2.400	2.266	1.966	1.623	1.317	1.076	0.895	0.754
3-4	4.248	4.196	4.355	4.356	4.051	3.547	3.012	2.555	2.216	1.982	1.810
Mn IV	3.8	4.0	4.2	4.4	4.6	4.8	5.0	5.2	5.4	5.6	5.8
0-1	1.896	1.753	1.494	1.209	0.959	0.764	0.625	0.531	0.469	0.422	0.377
0-2	1.396	1.188	0.937	0.704	0.516	0.379	0.284	0.221	0.182	0.158	0.143
0-3	1.145	0.942	0.724	0.531	0.380	0.271	0.196	0.146	0.112	0.088	0.069
0-4	1.572	1.254	0.942	0.682	0.487	0.348	0.252	0.188	0.143	0.110	0.085
1-2	4.454	3.894	3.180	2.505	1.956	1.551	1.271	1.088	0.967	0.877	0.789
1-3	4.144	3.450	2.672	1.976	1.429	1.031	0.758	0.577	0.457	0.377	0.318
1-4	2.411	2.023	1.610	1.239	0.941	0.715	0.551	0.434	0.349	0.283	0.226
2-3	5.734	4.958	4.060	3.222	2.543	2.046	1.708	1.490	1.347	1.240	1.131
2-4	5.719	4.725	3.740	2.880	2.183	1.645	1.248	0.964	0.761	0.613	0.495
3-4	9.346	8.038	6.660	5.370	4.257	3.360	2.683	2.200	1.864	1.621	1.417
Fe V	4.0	4.2	4.4	4.6	4.8	5.0	5.2	5.4	5.6	5.8	6.0
0-1	0.861	0.728	0.609	0.515	0.447	0.400	0.370	0.350	0.331	0.308	0.274
0-2	0.461	0.367	0.285	0.221	0.176	0.146	0.127	0.115	0.109	0.105	0.102
0-3	0.392	0.301	0.224	0.167	0.126	0.098	0.079	0.060	0.056	0.047	0.038
0-4	0.338	0.256	0.193	0.149	0.118	0.097	0.082	0.070	0.060	0.051	0.042
1-2	2.438	1.951	1.553	1.256	1.048	0.909	0.820	0.761	0.713	0.660	0.591
1-3	1.441	1.107	0.833	0.628	0.484	0.386	0.322	0.279	0.249	0.226	0.204
1-4	1.265	0.941	0.698	0.524	0.405	0.323	0.267	0.226	0.192	0.161	0.132
2-3	3.214	2.615	2.114	1.733	1.462	1.279	1.161	1.083	1.020	0.952	0.864
2-4	2.427	1.808	1.339	1.004	0.773	0.618	0.513	0.440	0.383	0.333	0.285
3-4	6.727	5.070	3.788	2.862	2.223	1.801	1.529	1.352	1.226	1.117	1.003
Co VI	4.2	4.4	4.6	4.8	5.0	5.2	5.4	5.6	5.8	6.0	6.2
0-1	0.403	0.361	0.334	0.316	0.305	0.298	0.292	0.283	0.267	0.242	0.208
0-2	0.117	0.104	0.096	0.091	0.088	0.086	0.085	0.085	0.085	0.084	0.082
0-3	0.062	0.055	0.051	0.047	0.045	0.043	0.041	0.038	0.034	0.030	0.024
0-4	0.056	0.053	0.051	0.049	0.048	0.047	0.044	0.041	0.037	0.032	0.026
1-2	0.824	0.750	0.705	0.670	0.646	0.629	0.615	0.595	0.562	0.513	0.447
1-3	0.340	0.313	0.288	0.265	0.243	0.225	0.210	0.196	0.183	0.169	0.154
1-4	0.216	0.201	0.189	0.178	0.167	0.157	0.146	0.134	0.119	0.101	0.083
2-3	1.311	1.236	1.165	1.097	1.035	0.982	0.936	0.890	0.835	0.763	0.674
2-4	0.592	0.523	0.469	0.423	0.384	0.351	0.321	0.293	0.264	0.233	0.200
3-4	1.380	1.260	1.174	1.110	1.062	1.025	0.992	0.954	0.904	0.835	0.744
Ni VII	4.4	4.6	4.8	5.0	5.2	5.4	5.6	5.8	6.0	6.2	6.4
0-1	0.345	0.326	0.309	0.294	0.282	0.272	0.260	0.244	0.220	0.191	0.156
0-2	0.692	0.519	0.426	0.335	0.257	0.198	0.156	0.127	0.107	0.094	0.084
0-3	0.391	0.336	0.271	0.209	0.156	0.116	0.086	0.064	0.048	0.036	0.026
0-4	0.047	0.046	0.044	0.042	0.040	0.038	0.035	0.032	0.027	0.023	0.019
1-2	0.550	0.536	0.530	0.529	0.529	0.527	0.516	0.492	0.453	0.400	0.335
1-3	0.309	0.285	0.258	0.232	0.210	0.192	0.176	0.162	0.149	0.136	0.122
1-4	0.121	0.121	0.120	0.119	0.116	0.112	0.105	0.096	0.084	0.070	0.057
2-3	0.870	0.848	0.827	0.809	0.794	0.778	0.754	0.717	0.663	0.593	0.511
2-4	0.249	0.249	0.248	0.246	0.242	0.236	0.226	0.210	0.190	0.168	0.144
3-4	0.850	0.848	0.847	0.846	0.844	0.835	0.816	0.781	0.728	0.658	0.575